Supplementary Information for

Microbial influx during early postnatal life fortifies the ocular surface and guards against allergic eye disease in mice

Yanbo Liu, Hang Sun, Shulin Song, Xiezhou He, Han Wu, Shangkun Ou, Hui He, Rongrong Zong, Yongxiong Chen, Guo Fu, Yiqiang Wang, Huping Wu, Andrew J. Quantock, Zuguo Liu, and Wei Li

Wei Li
Email: wei1018@xmu.edu.cn.

This file includes:

Supplementary materials and methods

DNA extraction, amplification of 16S rRNA and sequencing

The conjunctival tissue and feces samples were separately thawed on ice and homogenized in liquid nitrogen. Genomic DNA from different samples was extracted using a QIAamp DNA Mini Kit and a QIAamp DNA Stool Mini Kit (Qiagen, Hilden, Germany), respectively. To ensure complete lysis, the manufacturer's protocol was modified with the addition of 3.2 µl freshly prepared lysozyme (10 mg/ml) (Sigma-Aldrich, Merck KGaA, Darmstadt, Germany) to the lysis buffer. The solution was briefly vortexed then incubated at 37°C for 30 min. Then, 20 µl Proteinase K (20 mg/ml) was added to the solution, vortexed, incubated at 56 °C for 1-3 hours and vortexed again. The manufacturer's protocol was then followed. The quality and quantity of DNA were determined by 1.0% agarose gel electrophoresis and a NanoDrop® ND-2000 spectrophotometer (Thermo Scientific Inc., USA). The DNA was stored at -80 °C prior to further use.

The V3-V4 region of the 16S rRNA gene was amplified and sequencing was performed at Gene Denovo Biotechnology Co., Ltd (Guangzhou, China). Laboratory environmental samples along with blank extractions and reagents used at the time of amplification were also processed and analyzed as potential sources of contamination. The primers used were as follows: 341F (5'- CCTACGGGNGGCWGCAG-3') and 806R (5'-GGACTACHVGGGTATCTAAT-3'). PCR reactions were performed in triplicated 50 µl mixture containing 10µl of 5×Q5@ Reaction Buffer, 10µL of 5×Q5@ High GC Enhancer, 1.5 µl of 2.5 mM dNTPs, 1.5 µl of each primer (10 µM), 0.2µL of Q5@ High-Fidelity DNA Polymerase and 50 ng template DNA. The reaction condition comprised an initial denaturation at 95°C for 5 min followed by 30 cycles at 95°C for 1 min and 72°C for 1 min and a final extension at 72°C for 7 min.

The PCR product was extracted from 2% agarose gel and purified using the AxyPrep DNA Gel Extraction Kit (Axygen Biosciences, Union City, CA, U.S.A) according to the manufacturer's instructions and quantified using ABI StepOnePlus Real-Time PCR system (Life Technologies, Foster City, USA). Purified amplicons were pooled in equimolar and paired end sequenced (PE250) on an Illumina platform according to the standard protocols.

Data processing

Raw FASTQ files were de-multiplexed using an in-house perl script, and then quality-filtered by Fastp (v0.18.0). High-quality data were obtained and overlapped with tags using

FLASH (v1.2.11) with a minimum overlap of 10 bp and mismatch error rates of 2%. The optimized sequences were then clustered into operational taxonomic units (OTUs) using UPARSE (v9.2.64) with 97% identity threshold. All chimeric tags were removed using the UCHIME algorithm to finally obtain effective tags for further analysis. Representative sequences of OTUs were classified into organisms by a naive Bayesian model using RDP classifier (v 2.2) based on SILVA database (v132). The confidence threshold was set to 0.8.

TUNEL assay

TUNEL assay was performed on frozen sections using the Dead End Fluorometric TUNEL System (G3250, Promega) according to the manufacturer's instructions. Sections were counterstained with DAPI, mounted and photographed with a laser scanning confocal microscope (FV1000MPE-B, Olympus). Positive and negative controls were included in the analysis.

Immunohistochemical staining

Paraffin sections were rehydrated and blocked with 3% hydrogen peroxide for 10 min. They were then washed with PBS and incubated in Triton X-100 (0.2%). After washing again, the sections were incubated with BSA (2%) for 1 h, and following a rinse were incubated overnight at 4°C with anti-CD4 antibody (1:200). The next day, the sections were incubated with biotinylated anti-rabbit IgG (1:50) for 1 h after rinsing, followed by Vectastain Elite ABC reagent for 30 min. The reaction product was then developed with diaminobenzidine (DAB), and examined under a light microscope (Eclipse 50i; Nikon, Tokyo, Japan).

Conjunctival cultures

Explants were excised from the forniceal conjunctiva of 2-week-old C57BL/6J mice and incubated in supplemental hormonal epithelial medium (SHEM; Gibco, C11330500BT, USA) supplemented with 5% fetal bovine serum (ABW, 0827555, Shanghai, China), 1.0 mg/ml insulin (Procell, PB180431, Wuhan,China), 0.55mg/ml transferrin (Procell, PB180431, Wuhan, China), 0.5 μg/ml hydrocortisone (Yeasen, 40109ES08, Shanghai, China). Conjunctival explants were plated, one explant per well, in 48-well plates and received 200 μl per week of either SHEM with 10 μM Y27632 (MCE, HY-10071) or SHEM with 10 μM Y2763 supplemented with 0.03 mg/ml, 0.3 mg/ml and 3 mg/ml tobramycin (Sangon Biotech, Shanghai, China). Cultures were incubated for 7 days. Subsequently

cell proliferation/viability was assessed (Millipore, USA), with cultures fixed in cold methanol and immunostained.

WST-1 assay

After 7 days, media and explants were removed and new media supplemented with cell proliferation reagent WST-1 (Millipore, USA) at a final concentration (1:10) was added, after which culture plates were placed in an incubator at 37 °C. After 6- or 24-hours absorbance, delta was measured at wavelengths 440 and 690 nm using a spectrophotometer (Thermo Fisher, USA).

Supplementary tables

Table S1. Summary statistics of 16S rRNA gene sequencing

Samples	N	Clean tags	Effective tags	Average of effective tags per samples	Coverage range	OTUs	Average of OTUs
Conjunctival samples							
1w	10	1158361	1106805	110680.50	89.36	5867	586.7
2w	10	1108679	1053281	105328.10	86.80	7254	725.4
3w	10	1168612	1118078	111807.80	89.42	7098	709.8
4w	10	1045157	985273	98527.30	89.42	5945	594.5
6w	10	1053992	998860	99886.00	88.74	6487	648.7
8w	10	1147278	1097323	109732.30	89.82	6115	611.5
Total	60	6682079	6359620	105993.67	88.93	38766	646.1
Environmental samples							
E-1w	3	365614	319277	106425.67	81.89	2193	731.00
E-2w	3	320647	283338	94446.00	82.48	2215	738.33
E-3w	3	338074	295257	98419.00	81.86	2082	694.00
E-4w	3	345054	299549	99849.67	81.45	2309	769.67
E-6w	3	356199	317755	105918.33	83.59	2201	733.67
E-8w	3	348770	313532	104510.67	84.22	1716	572.00
Total	18	2074358	1828708	10159.89	82.58	12716	706.44
Conjunctival samples （Topic antibiotic/saline exposure）							
C-3w	10	1162197	1110753	111075.30	93.26	7142	714.20
C-4w	10	1020834	980646	98064.60	94.80	6129	612.90
C-5w	10	1279860	1215109	121510.90	93.52	9339	933.90
T-3w	10	1280095	1241075	124107.50	95.47	6326	632.60
T-4w	10	1283377	1240049	124004.90	95.16	6075	607.50
T-5w	10	1280805	1252298	125229.80	96.22	5035	503.50
Total	60	7307168	7039930	117332.17	94.74	40046	667.43
Negative samples							
NC	3	274848	240532	80177.33	86.09	1110	370

Table S2. Discriminating genus in conjunctiva between different growth stages using SIMPER

Genus	Contribution	Cumulative contribution
1w vs 2w		
Staphylococcus	0.22834083	0.30079610
Acinetobacter	0.22081747	0.59168158
Enterococcus	0.17381004	0.82064362
Anoxybacillus	0.13615331	1
2w vs 3w		
Enterococcus	0.31704422	0.47126038
Staphylococcus	0.26360680	0.86309040
Acinetobacter	0.06347564	0.95744176
Anoxybacillus	0.02863140	1
3w vs 4w		
Enterococcus	0.31704422	0.47126038
Staphylococcus	0.26360680	0.86309040
Acinetobacter	0.06347564	0.9574416
Anoxybacillus	0.02863140	1

Table S3. Topological properties of co-occurring bacterial networks obtained among six groups (1w, 2w, 3w, 4w, 6w, 8w)

Network metrics	Total bacterial community					
Empirical networks	**1w**	**2w**	**3w**	**4w**	**6w**	**8w**
Number of nodes	52	36	47	48	66	53
Number of edges	240	128	149	287	340	281
Number of positive correlations	90%	93.75%	91.28%	94.77%	88.82%	92.88%
Number of negative correlations	10%	6.25%	8.72%	5.23%	11.18%	7.12%
Average path length (APL)	2.725	2.499	3.44	2.385	2.628	2.561
Graph Density	0.181	0.203	0.138	0.254	0.159	0.204
Network diameter	7	5	8	7	6	6
Average clustering coefficient (avgCC)	0.626	0.532	0.615	0.689	0.628	0.638
Average degree (avgK)	9.231	7.111	6.34	11.958	10.303	10.604
Modularity (M)	0.509	0.481	0.736	0.364	0.526	0.378
Average Weighted Degree	6.268	5.084	4.551	11.124	6.767	8.095

Table S4. Topological properties of co-occurring bacterial networks obtained among four groups (C-4w, T-4w, C-5w, T-5w)

Network metrics	Total bacterial community			
Empirical networks	**C-4w**	**T-4w**	**C-5w**	**T-5w**
Number of nodes	110	189	214	120
Number of edges	791	1424	1788	704
Number of positive correlations	93.55%	68.82%	73.1%	66.05%
Number of negative correlations	6.45%	31.18%	26.9%	33.95%
Average path length (APL)	2.516	2.636	2.572	2.979
Graph Density	0.132	0.08	0.078	0.098
Network diameter	5	5	5	8
Average clustering coefficient (avgCC)	0.542	0.466	0.446	0.575
Average degree (avgK)	14.382	15.069	16.71	11.733
Modularity (M)	0.525	1.398	1.04	1.848
Average Weighted Degree	10.006	4.71	6.199	3.776

Table S5. List of immunofluorescence and flow cytometry antibodies

Antibodies	Source	Identifier
Immunofluorescent and Immunohistochemical Staining		
CD45	Santa Cruz	sc-52491
CD11b	Abcam	ab8878
CD11c	BD Pharmingen	550283
MHC Class II	Abcam	ab25333
Keratin 7 (Krt7)	Santa Cruz	sc-53263
CD4	Abcam	ab183685
Ki67	Abcam	ab16667
ZO-1	Invitrogen	61-7300
Keratin 19 (Krt19)	Abcam	ab52625
Secondary antibodies:		
Donkey Anti-Rat AF594	Invitrogen	A-21209
Donkey Anti-Rat AF488	Invitrogen	A-21208
Donkey Anti-Mouse AF594	Invitrogen	A-21203
Donkey Anti-Rabbit AF488	Abcam	ab150073
Donkey Anti-Rabbit AF647	Abcam	ab150075
Goat Anti-Armenian Hamster AF488	Jackson ImmunoResearch	127-545-160
Flow cytometry		
CD45_BV421, clone 30-F11	BD Pharmingen	563890
CD3_APC, clone 145-2C11	BD Pharmingen	561826
CD4_FITC, clone GK1.5	BD Pharmingen	553729
CD25_PerCP, clone PC61	BioLegend	102027
Foxp3_PE, clone MF23	BD Pharmingen	560414
IL-4_BV605, clone 11B11	BioLegend	504126
IFN-γ_BV650, clone XMG1.2	BioLegend	505832
Fixable viability stain 780	BD Pharmingen	565388

Table S6. Sequences used for quantitative Real-Time PCR

Gene Name	Sense Primer	Antisense Primer
β-actin	5'-GCTGTATTCCCCTCCATCGT-3'	5'-CTTCTCCATGTCGTCCCAGT-3'
Muc5ac	5'-TGGCACCTGCTCAGTAATGG-3'	5'-TCCGTCAGTCCACACTTTCG-3'
Ki67	5'-CACTCCAAAGAAACCCACAA-3'	5'-CTCATCTGCTGCTGCTTCTC-3'
Krt19	5'-GACATAGAGCGCCAGAACCA-3'	5'-GGCAGATTGTTGTAGTGGGC-3'
Tjp1(Zo-1)	5'-GATGAGCGGGCTACCTTACTgG-3'	5'-TCCACTGCTTTGGGTGGAT-3'
H2-Ab1	5'-AGGGCATTTCGTGTACCAGTT-3'	5'-GTACTCCTCCCGGTTGTAGATGTA-3'
Gata3	5'-TTTACCCTCCGGCTTCATCCTCCT-3'	5'-TGCACCTGATACTTGAGGCACTCT-3'
IL-4	5'-ATCATCGGCATTTTGAACGAGG-3'	5'-TGCAGCTCCATGAGAACACTA-3'
IL-5	5'-TCAGGGGCTAGACATACTGAAG-3'	5'-CCAAGGAACTCTTGCAGGTAAT-3'

Supplementary figures and legends

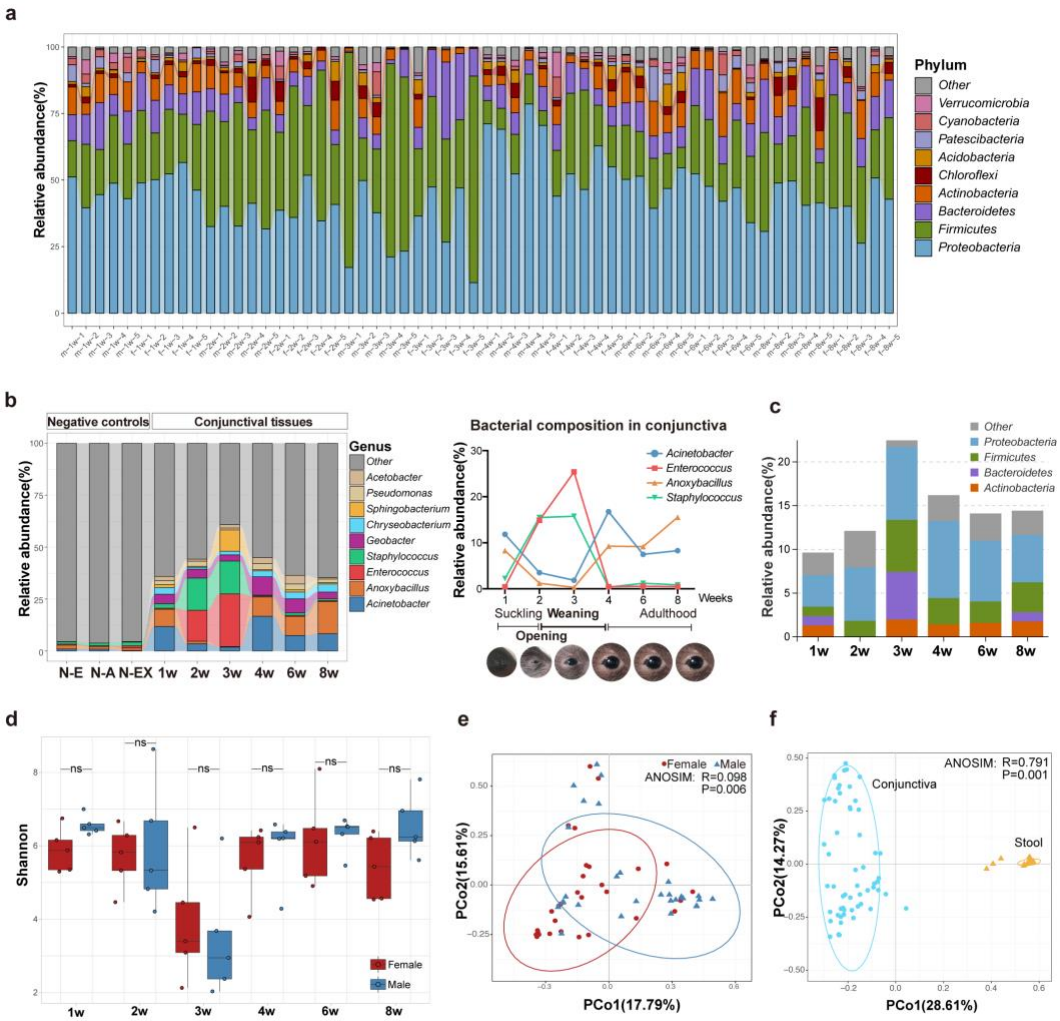

Fig. S1 Composition of the mouse ocular surface microbiome at genus level and sex-differences in the conjunctival microbiome. a Distribution of abundant bacterial phyla (top 10) in all 60 samples across different growth stages. **b** Distribution of abundant bacterial genus (top 10) across different growth stages (n=10 per group). Negative controls include laboratory environmental samples (N-E), reagents used at the time of amplification (N-A) and blank extractions (N-EX). **c** BugBase prediction of potential pathogenic bacteria of in conjunctiva across the different developmental stages in mice. **d** Shannon index with dot plots and box plots across different stages in female or male mice. **e f** Principal coordinate analysis plot generated using operational taxonomic unit (OTU) metrics based on the Bray-Curtis dissimilarities. Each point represents a sample. Error bars represent mean ± SEM. ns P>0.05 using the two-tailed Student's t-test (**d**).

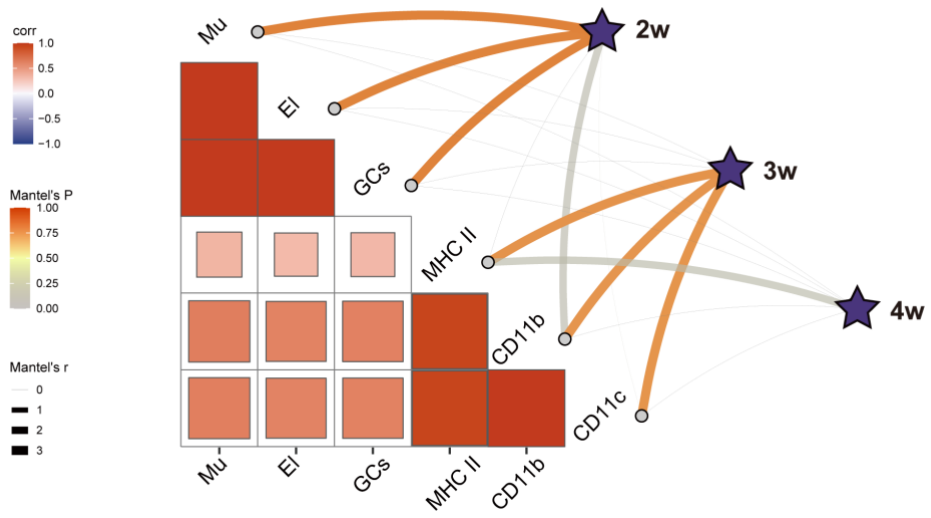

Fig. S2 Correlation between the conjunctival microbiome and conjunctival states. The correlation between ocular surface microbial communities (Bray-Curtis distance) and parameters of conjunctival states in 2-, 3- and 4-week-old mice was analyzed with using Mantel tests. The edge width corresponds to the R-value and the edge color denotes the statistical significance. The color gradient indicates Pearson correlation coefficients among the clinical parameters. Mu, *Muc5ac* mRNA expression level; El, conjunctival epithelial layers; GCs, the number of conjunctival goblet cells; CD11b, CD11c, MHC II, the percentage of deep intraepithelial APCs.

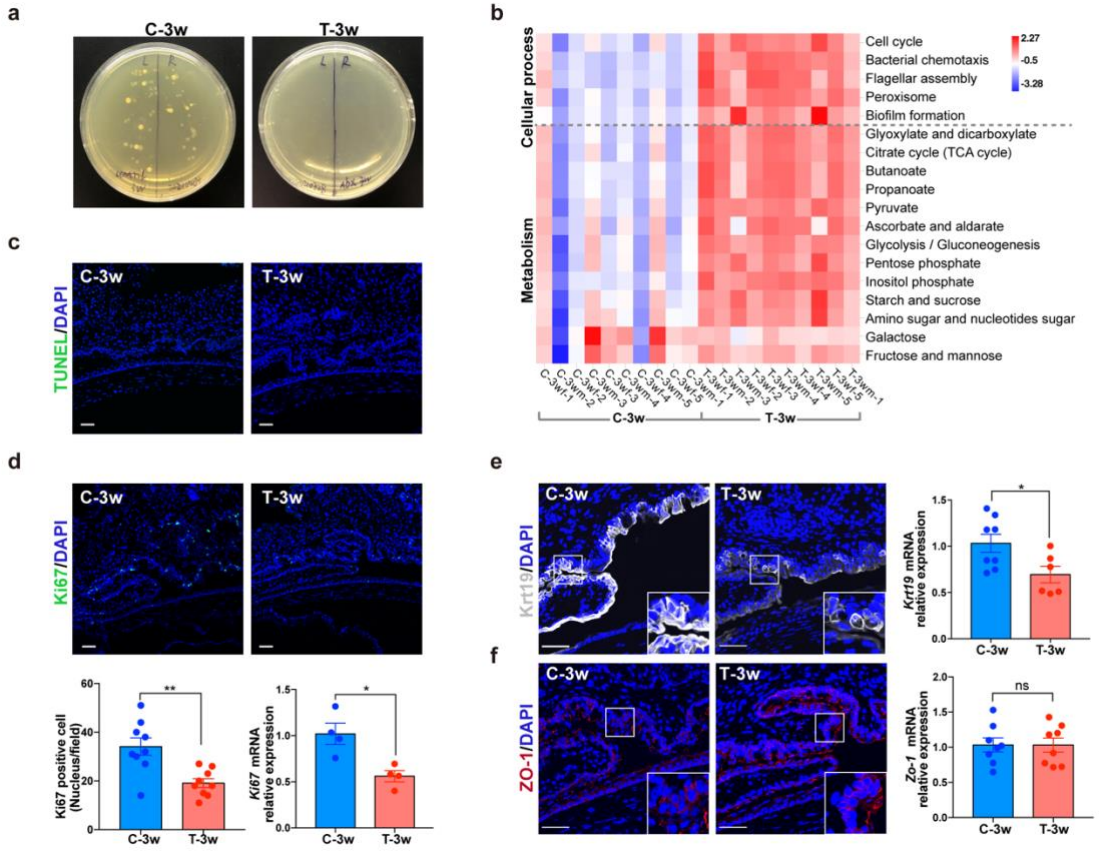

Fig. S3 Topical antibiotic exposure in early postnatal life delays the maturation of the conjunctival epithelium. a Ocular surface bacteria isolation of saline-treated (Ctrl) and antibiotic-treated (Tob) mice treated between weeks 2 and 3 (C-3w, T-3w) cultured on BHI plates. **b** Heatmaps of PICRUSt2-inferred functions. Intensity represents the Z score normalized predicted relative abundance of pathways. **c** TUNEL assay of conjunctival sections of C-3w and T-3w mice using Dead End Fluorometric TUNEL System (green) and counterstained with DAPI (blue). **d** Immunofluorescence of conjunctival sections of C-3w and T-3w mice with a monoclonal antibody against Ki67 (green) and DAPI (blue). Bar graphs present the quantification of ki67 positive cells (n=9 per group) and *Ki67* mRNA expression in conjunctiva in each time point (n=4 per group). **e, f** Immunofluorescence of conjunctival sections of C-3w and T-3w mice with monoclonal antibodies against cytokeratin 19 (Krt19, grey), ZO-1 (red) and DAPI (blue). Bar graphs present the *Krt19* and *Zo-1* mRNA expression in conjunctiva of C-3w and T-3w mice (n=6-8 per group). Scale bar, 50 μm**.** Data are shown as mean ± SEM. ns $P>0.05$, *$P<0.05$, **$P<0.01$ using the unpaired t test.

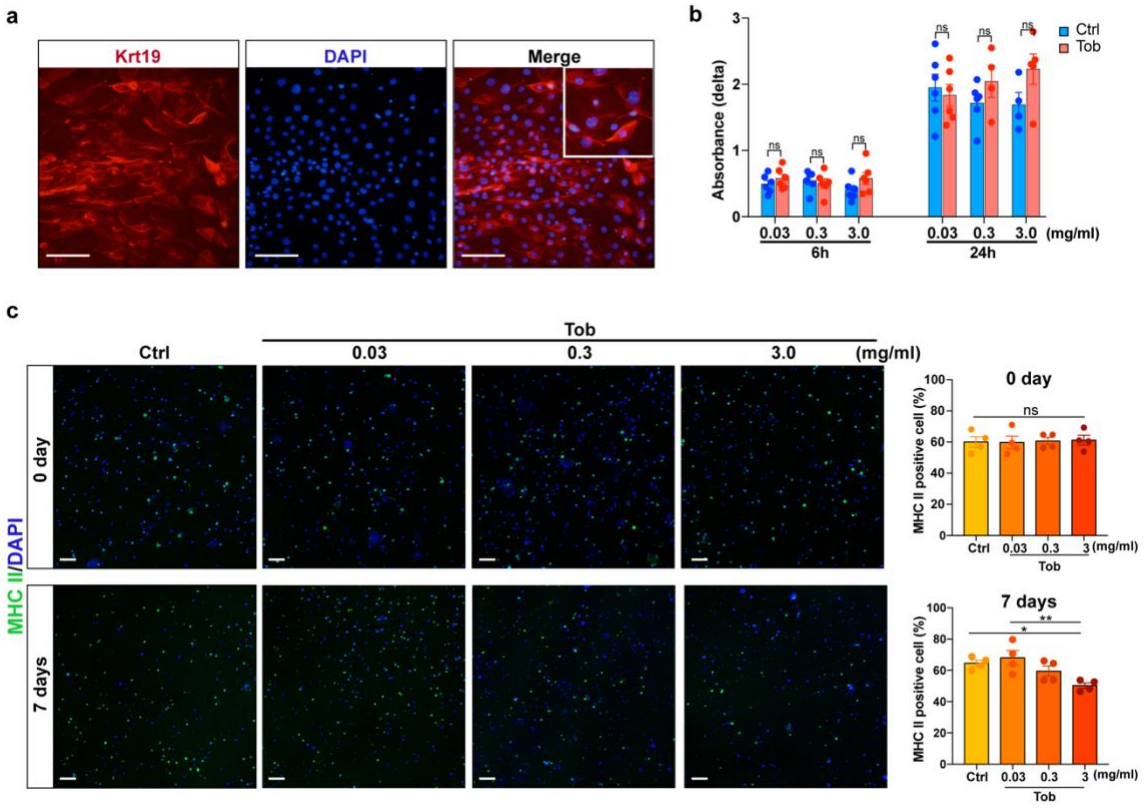

Fig. S4 Low concentrations of antibiotics have no direct effect on conjunctival cells proliferation and MHC II expression in CLN cells. a Immunofluorescence of control conjunctival explant cultures with monoclonal antibodies against cytokeratin 19 (Krt19, red) and Hoechst (blue). **b** Primary conjunctival cultures were incubated with increasing concentrations of tobramycin (Tob) for 7 days, and cell proliferation determined by WST assay (n=4-6 per group). **c** Immunofluorescence staining of CLN cells with monoclonal antibodies directed against MHC II (green) and DAPI (blue). The frequency of MHC II positive cells in CLN cells under different antibiotic concentrations (n=4 per group). Scale bar, 100 μm (**a**) and 50 μm (**c**). Data are shown as mean ± SEM. ns $P>0.05$, *$P<0.05$, **$P<0.01$ using the one-way ANOVA.

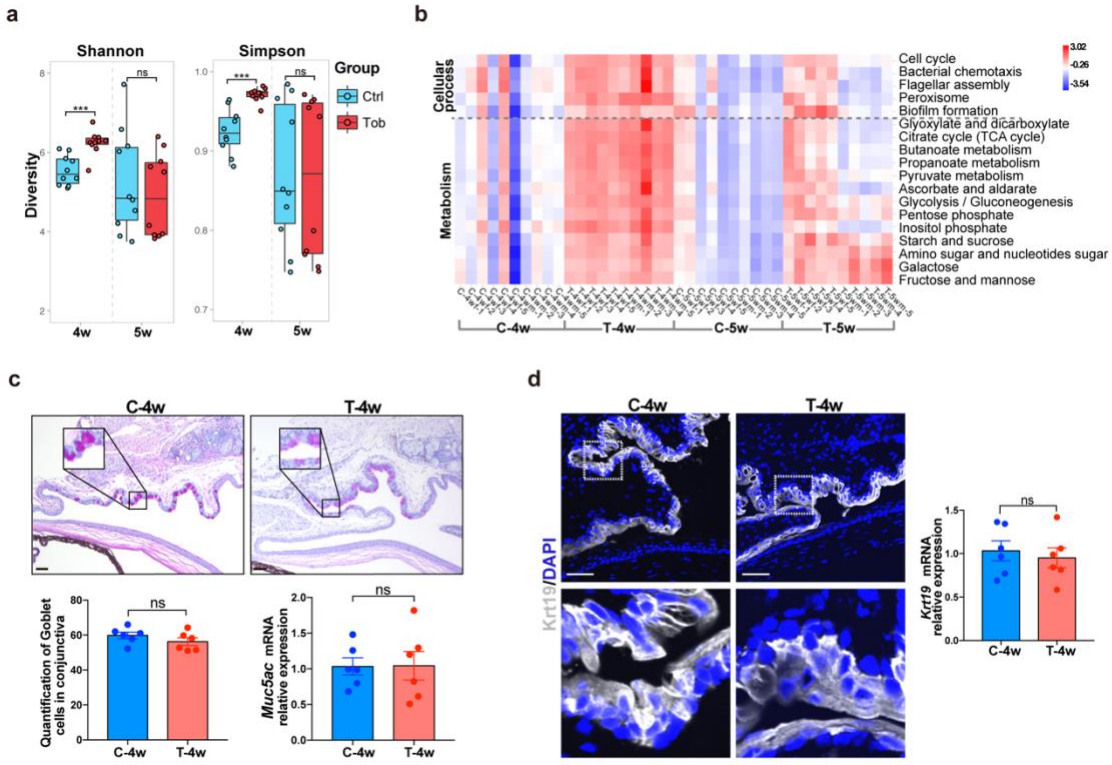

Fig. S5 The conjunctival tissue is recovering to homeostasis after discontinuing topical antibiotic exposure. a Shannon index and Simpson index with dot plots and box plots of the groups which discontinued antibiotic/saline use for 1 week (C-4w, T-4w) or 2 weeks (C-5w, T-5w) after topical antibiotic exposure for 1 week (n=10 per group). **b** Heatmaps of PICRUSt2-inferred functions. Intensity represents the Z score normalized predicted relative abundance of pathways. **c** Representative images of conjunctiva sections stained with PAS. Bar graphs present the quantification of goblet cells and *Muc5ac* mRNA expression in conjunctiva in C-4w and T-4w mice (n=6 per group). **d** Immunofluorescence of conjunctiva sections of C-4w and T-4w mice with a monoclonal antibody against cytokeratin 19 (Krt19, grey) and DAPI (blue). Bar graphs present the *Krt19* mRNA expression in conjunctiva in each time point (n=6 per group). Scale bar, 50 μm. Data are shown as mean ± SEM. ns $P>0.05$, ***$P<0.001$ using the unpaired t test.

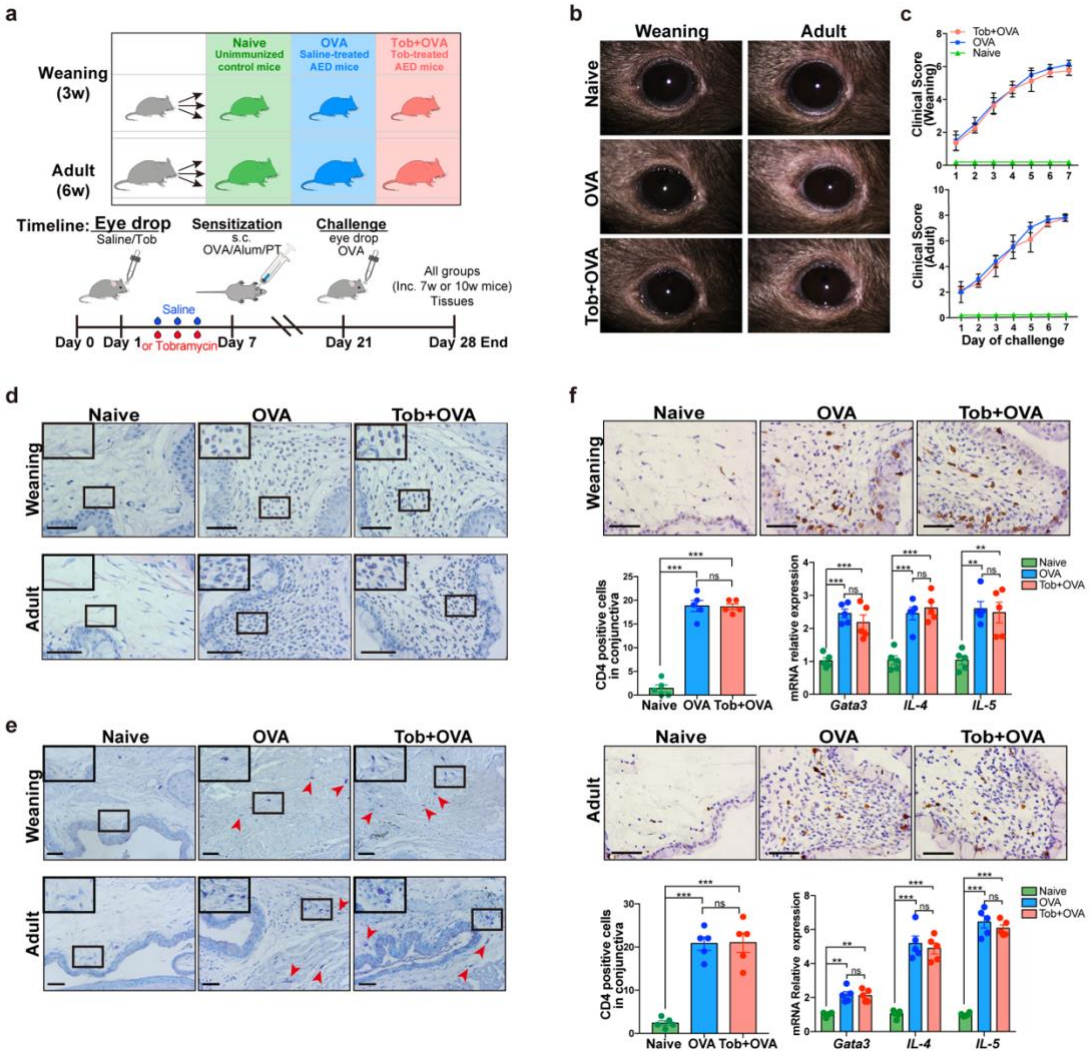

Fig. S6 The absence of aggravated AED in weaning and adult mice after topical antibiotic exposure. a Mouse grouping strategy and study design for inducting AED after 1 week of topical antibiotic exposure in weaning or adult mice. **b, c** Clinical manifestations and clinical scores of naive untreated mice, OVA mice and Tob+OVA mice in weaning and adult groups (n=5 per group). **d** Eosinophilic infiltration. Black squares are magnified on the top left. **e** Mast cells (MCs) were stained by toluidine blue. Black squares are magnified on the top left. **f** Immunohistochemistry of conjunctival sections in naive, OVA and Tob+OVA groups with a monoclonal antibody against CD4. Bar graphs present the quantification of CD4 positive cells, as well as *Gata3*, *IL-4 and IL-5* mRNA expression in conjunctiva of each group (n=5 per group). Scale bar, 50 μm. Data are shown as mean ± SEM. ns $P>0.05$, ** $P<0.01$, *** $P<0.001$ using the one-way ANOVA.

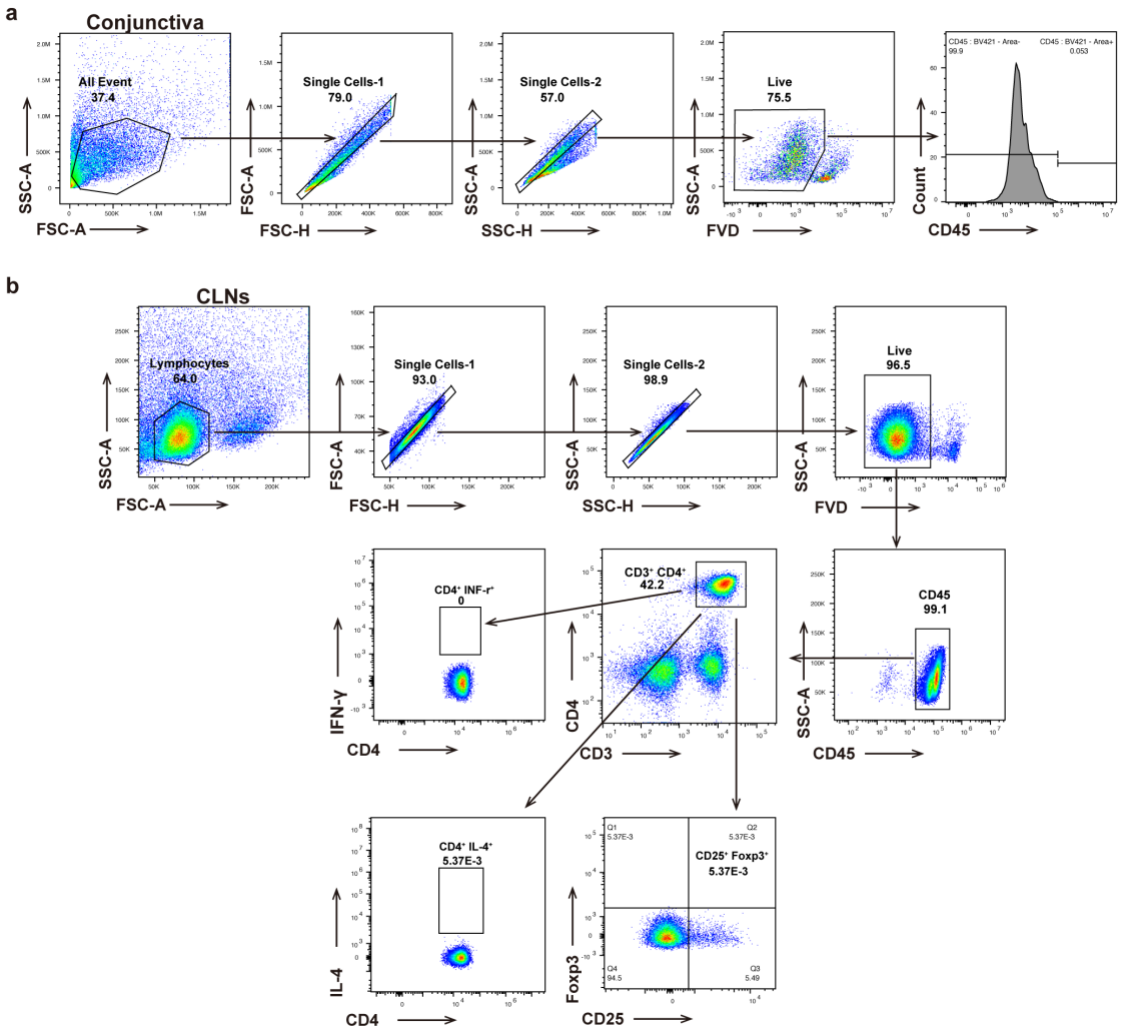

Fig.S7 Gating strategies for flow cytometry experiments. a Representative flow cytometry gating strategy for $CD45^+$ cells in conjunctiva from 1- to 4-week-old mice. **b** Gating strategy for assessing Th1 ($CD4^+$ IFN-γ^+), Th2 ($CD4^+$ IL-4^+) and Treg ($CD4^+$ $CD25^+$ $Foxp3^+$) cells in CLNs of naive, OVA and Tob+OVA groups.